THE JOURNAL OF PHYSICAL CHEMISTRY C

Article

pubs.acs.org/JPCC

Controlling the Electronic Properties of Nanodiamonds via Surface Chemical Functionalization: A DFT Study

Noam Brown and Oded Hod*

Department of Chemical Physics, School of Chemistry, The Raymond and Beverly Sackler Faculty of Exact Sciences, Tel-Aviv University, Tel-Aviv 69978, Israel

Supporting Information

ABSTRACT: The electronic properties of chemically functionalized nanodiamonds are studied using density functional theory calculations. HOMO−LUMO gaps and relative stabilities are calculated for different surface functionalization schemes and diamond nanocrystal morphologies. The effects of chemical decoration on the size and nature of the HOMO−LUMO gap of the various systems considered are discussed in detail. We conclude that surface chemical functionalization has the potential to become an accessible route for controlling the electronic properties of nanodiamonds.

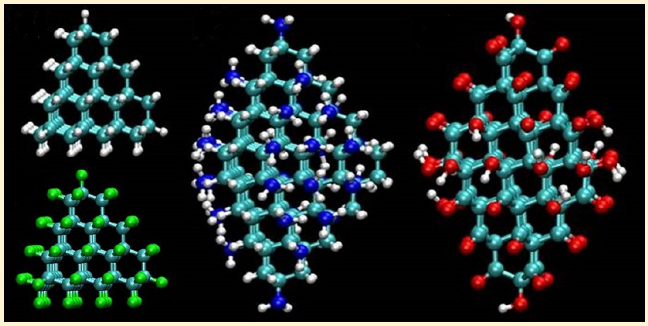

INTRODUCTION

Carbon-based nanocrystalline materials may form a diverse array of lattice structures ranging from (quasi-)zero-dimensional nanodots through (quasi-)one-dimensional nanotubes and nanowires, and two-dimensional sheets, to three-dimensional crystal structures.[1−4] This is a result of the flexibility of the carbon atom in forming two (sp hybridization), three (sp^2 hybridization), and four (sp^3 hybridization) carbon−carbon bonds. This diversity provides an excellent platform for material engineering[5] allowing for delicate control over their physical and chemical properties and opening the door for fascinating technological applications in many fields including electronics,[6,7] biology,[8,9] medicine,[10] and chemical catalysis.[11]

Specifically, nanodiamonds[12,13] have become a focus of extensive study due to advances in synthesis techniques, such as chemical vapor deposition (CVD) and detonation synthesis.[14,15] It has been shown that nanodiamonds can coexist along with bucky-diamonds (carbon-onions), when annealed at high temperatures or treated by electron beam radiation.[16−25] Here, the outer surfaces of the diamond nanocrystals undergo a graphitization process, forming a carbon-onion structure, as a transition from sp^3 to sp^2 type bonds occurs. This graphitization process, which occurs due to dangling bonds appearing at the diamond's outer surfaces, was observed both experimentally[16−18] and theoretically.[19−25] The same studies have also shown that hydrogenation of the nanodiamond surfaces may prevent such graphitization by the elimination of the dangling bonds thus stabilizing the crystal structure.

Recently, chemical doping of nanodiamonds has been studied extensively aiming to control their physical properties and enable the design of nanoscale diamond-based semiconductors[26] and fluorescent biomarkers[8,9] with desired physical properties.[27−30] Apart from chemical doping, several experimental studies have addressed the issues of surface functionalization[31] exploring the possibility to enhance solubility in polar organic solvents and reduce aggregation of the nanoparticles in physiological conditions,[32] as well as to create platforms for catalysis and linkage to organic and bioorganic materials.[33,34] Despite these experimental efforts and the large body of computational work addressing the issue of nanodiamond chemical doping, to the best of our knowledge, first-principles studies on surface chemical functionalization of nanodiamonds have been relatively sparse.[35−38]

In the present article, we present the results of a density functional theory (DFT) study of the electronic properties and the heat of formation of carbon nanodiamonds of four different nanocrystal morphologies and several surface functionalization schemes. We find that both the HOMO−LUMO gap and the heat of formation are affected greatly by the type of chemical functionalization thus opening a new route for designing control schemes for the fabrication of nanodiamonds with desired physical properties.

The article is organized as follows: in the next section, we describe the diamond nanocrystal structures and the surface functionalization schemes that are considered. Next, we describe the computational methods used to perform the calculations and present our main results. This is followed by a discussion and conclusions of the present work.

Received: September 16, 2013
Revised: February 11, 2014
Published: February 12, 2014

   dx.doi.org/10.1021/jp409236t | J. Phys. Chem. C 2014, 118, 5530−5537

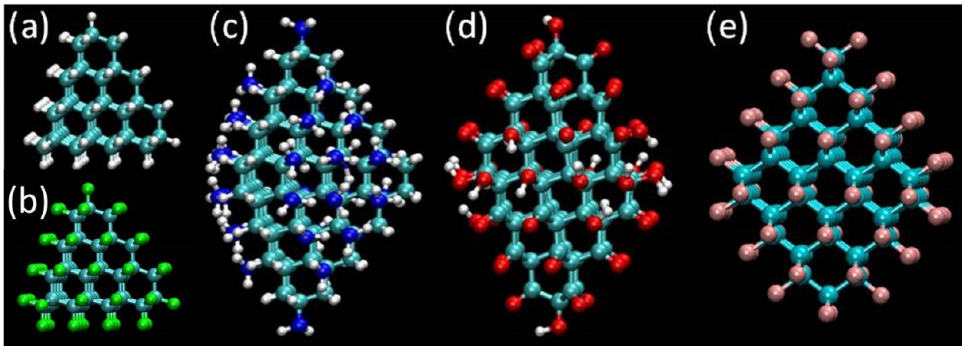

Figure 1. Schematic representation of the different nanodiamond structures considered in this work and some representative functionalization schemes. (a) Fully hydrogenated ND-I. (b) Fully chlorinated ND-I. (c) A partial nitrogenation scheme of ND-II. (d) Fully oxidized ND-III. (e) Fully fluorinated ND-IV. Cyan, gray, green, blue, red, and pink balls stand for carbon, hydrogen, chlorine, nitrogen, oxygen, and fluorine atoms, respectively.

NANODIAMOND STRUCTURES AND FUNCTIONALIZATION SCHEMES

Four different diamond nanocrystals were studied (see Figure 1): one tetrahedral C_{51} structure, marked as ND-I; two triangular bipyramid structures of C_{108} and C_{90}, marked as ND-II and ND-III, respectively; and one more traditional C_{84} octahedral structure, marked as ND-IV. The dimensions of the various nanocrystal structure considered were chosen to be sufficiently small in order to be able to exploit quantum confinement and edge chemistry effects on the electronic structure of the systems. We note that the nanodiamond cluster sizes studied herein (0.9−1.7 nm) are well within experimental reach, where nanodiamonds as small as 2 nm in size have been produced,[19,35] and correspond well to the dimensions of similar structures (C_{29}−C_{323}) previously considered in several computational studies.[21−23]

The tetrahedral structure (Figure 1a,b) is a triangular pyramid cut out of bulk diamond and functionalized at the outer surfaces. Triangular bipyramid ND-II (Figure 1c) is obtained by fusing two ND-I tetrahedrons at a given base. Triangular bipyramid ND-III (Figure 1d) is obtained by eliminating one atomic layer from one ND-I structure and fusing it to another ND-I structure such that the two pyramids are rotated to form a stacking fault of 120° with respect to each other. Octahedral structure ND-IV is a square bipyramid cut out of bulk diamond. The dangling bonds of each of the nanodiamonds considered were first entirely passivated with hydrogen atoms, followed by full structural relaxation. The obtained hydrogenated systems then served as reference for several functionalization schemes considered in this work including oxidation, nitrogenation, fluorination, chlorination, and carboxylation. These functionalization schemes were chosen for several reasons: oxygen and nitrogen are abundant in the atmosphere as well as in detonation synthesis environments and are thus likely to decorate the edges; surface fluorination and chlorination is known to stabilize nanoscale structures;[34,39] and carboxylic acid can be used as a linker for diamond,[40] nanodiamond,[32] and diamondoid systems.[41] Coordinates of the fully relaxed systems can be found in the Supporting Information.

ND-I was fully functionalized with fluorine, chlorine, and oxygen and partially functionalized (30%) with carboxylic acid and nitrogen. ND-II was fully hydrogenated and fluorinated and partially functionalized (30%) with all other substituents considered. ND-III was fully functionalized with hydrogen, fluorine, chlorine, oxygen, and nitrogen and partially functionalized (25%) with carboxylic acid. ND-IV was fully functionalized with fluorine, chlorine, nitrogen, and oxygen and partially functionalized (40%) carboxylic acid. Higher coverage schemes of the partially functionalized systems were not considered due to steric hindrance of the functionalizing group. In order to evaluate the gradual effects of partial functionalization, ND-I was hydrogenated and partially functionalized with chlorine (75%, 30%, and 7% coverage) and with oxygen (30%, and 7% coverage). A similar procedure was carried out for ND-III with nitrogen functionalization and oxidation (84%, 25%, and 10% coverage) and for ND-IV with chlorine, nitrogen, and oxygen (70%, 40%, and 12% coverage). When functionalizing the different nanodiamonds with oxygen and nitrogen containing groups, 3-fold coordinated carbon atoms (appearing at the lattice surfaces and the apexes) were decorated with a hydroxyl or a primary amine group and carbon atoms having a 2-fold coordination (appearing at the lattice edges) were decorated with a ketone or an imine (=NH) group.

COMPUTATIONAL METHODS

All calculations presented have been performed using density functional theory with three different exchange-correlation functional approximations including the local density approximation (LDA),[42−44] the Perdew−Burke−Ernzerhof (PBE) flavor of the generalized gradient approximation,[45,46] the screened-hybrid functional of Heyd, Scuseria, and Ernzerhof (HSE),[47−50] and the double-ζ polarized 6-31G** basis set[51,52] as implemented in the Gaussian09 suite of programs.[53] Convergence of the results with respect to the choice of basis set was validated with respect to calculations performed at the LDA/cc-pVTZ level of theory producing total energies and band gaps in agreement to within 10%. All considered structures have been fully optimized separately for each functional approximation and basis set used. Presented herein are the results obtained from the calculations performed using the HSE functional and the 6-31G** basis set; this approach has been shown to produce accurate structural and electronic properties of carbon-based nanostructures.[50,54−60] Whenever indicated, results of the LDA and PBE calculations and comparisons with the HSE results can be found in the Supporting Information.

HOMO−LUMO gap values reported were extracted from the difference between the highest occupied and lowest unoccupied Kohn−Sham orbitals. Calculations of the relative

dx.doi.org/10.1021/jp409236t | J. Phys. Chem. C 2014, 118, 5530−5537

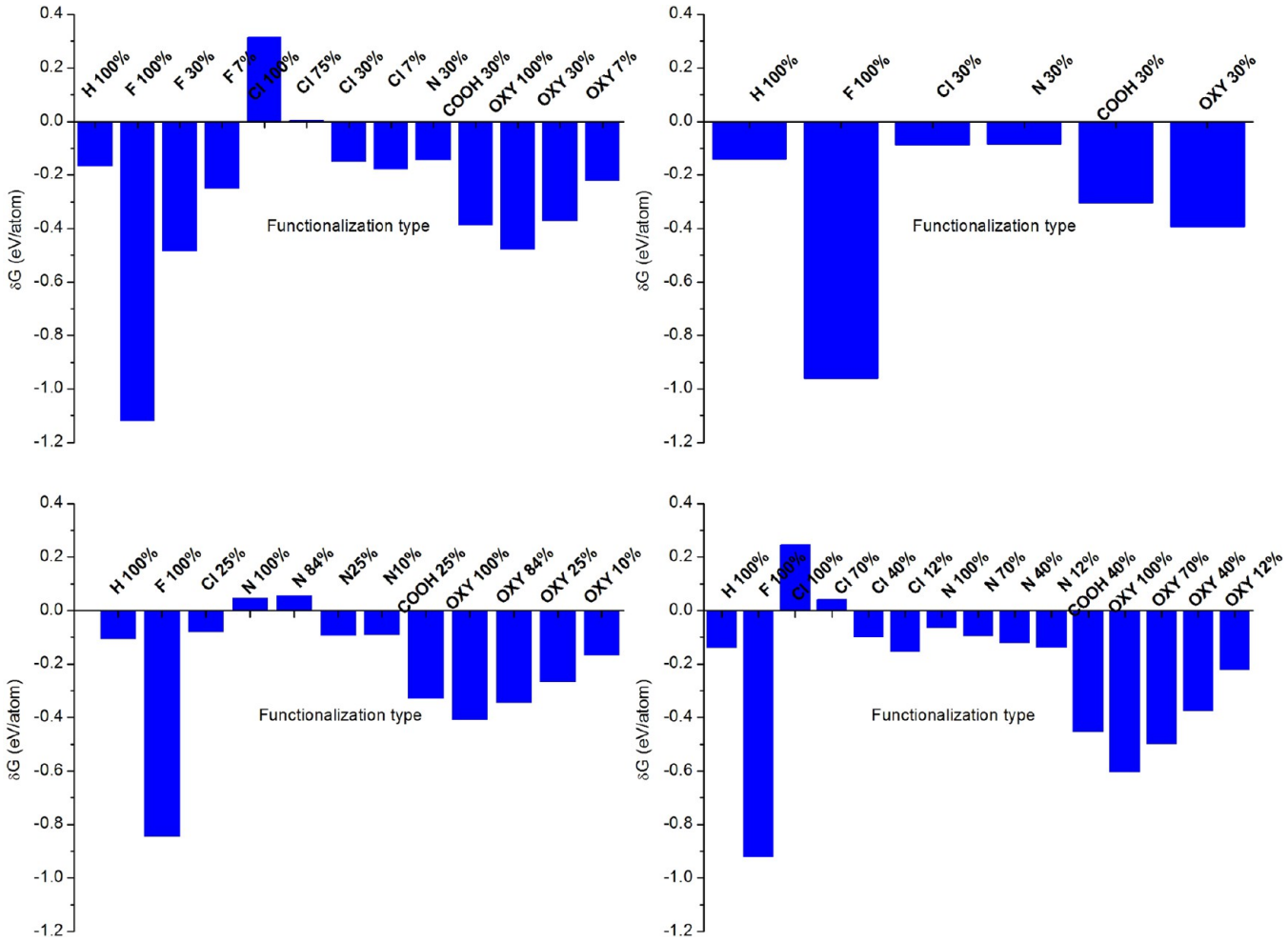

Figure 2. δG values, calculated using eq 1 at the HSE/6-31G** level of theory, for various surface functionalization schemes of the (a) ND-I, (b) ND-II, (c) ND-III, and (d) ND-IV systems.

stabilities of the different structures were performed using the following formula:[54,61]

$$\delta G = E - \chi_C \mu_{\text{diamond}} - \sum \chi_i \mu_i \quad (1)$$

Here, E is the cohesive energy per atom of the nanodiamond, χ_C is the molar fraction of the carbon atoms, μ_{diamond} is the chemical potential of the carbon atoms taken as the cohesive energy per atom of bulk diamond calculated at the same level of theory, χ_i is the molar fraction of the functionalizing atoms of type i, and μ_i is the chemical potential of the functionalizing atoms taken to be the binding energy per atom of each substituent in its natural form calculated at the same level of theory. For example, the chemical potential of oxygen was calculated as half the binding energy of the triplet state of an O_2 molecule. This definition allows for a direct energetic stability comparison between nanodiamonds of different chemical compositions, where negative values represent stable structures with respect to the constituents. It should be noted, however, that this treatment gives a qualitative measure of the relative stability while neglecting thermal and substrate effects and zero-point energy corrections.

RESULTS AND DISCUSSION

Relative Stability. We start by analyzing the relative stability of the various functionalization schemes of the different nanodiamond structures considered. In Figure 2, we present the relative stability of the different nanodiamonds, obtained using eq 1, as a function of the functionalization scheme calculated using the HSE functional approximation (results of the LDA and PBE calculations can be found in the Supporting Information). Focusing first on the results for the ND-I system (Figure 2a), we find that, compared to the hydrogen passivated systems (leftmost column); full surface fluorination is highly favored. We attribute this to the high electronegativity of the fluorine atoms making them excellent candidates to saturate the dangling surface carbon bonds. As may be expected, with decreasing fluorine surface coverages the stability of the ND-I structure reduces approaching that of the fully hydrogenated system. While a similar effect could be expected for chlorine atoms, at full coverage, the chlorinated system is found to be less stable than the hydrogenated one by 0.48 eV/atom. This may be attributed to the larger atomic volume of the chlorine atoms, leading to enhanced steric effects. This is further supported by the fact that at lower chlorine coverage schemes the relative stabilities of the systems increase monotonously. Partial nitrogenation (30%) results in structural stability comparable to that of the hydrogenated system, whereas partial carboxylation (30%) stabilizes the structure by 0.22 eV/atom. Similar to fluorination, full oxidation results in a stable structure, whereas lowering the oxygen coverage decreases the stability monotonously, to a change of 0.08 eV/atom (for

dx.doi.org/10.1021/jp409236t | J. Phys. Chem. C 2014, 118, 5530−5537

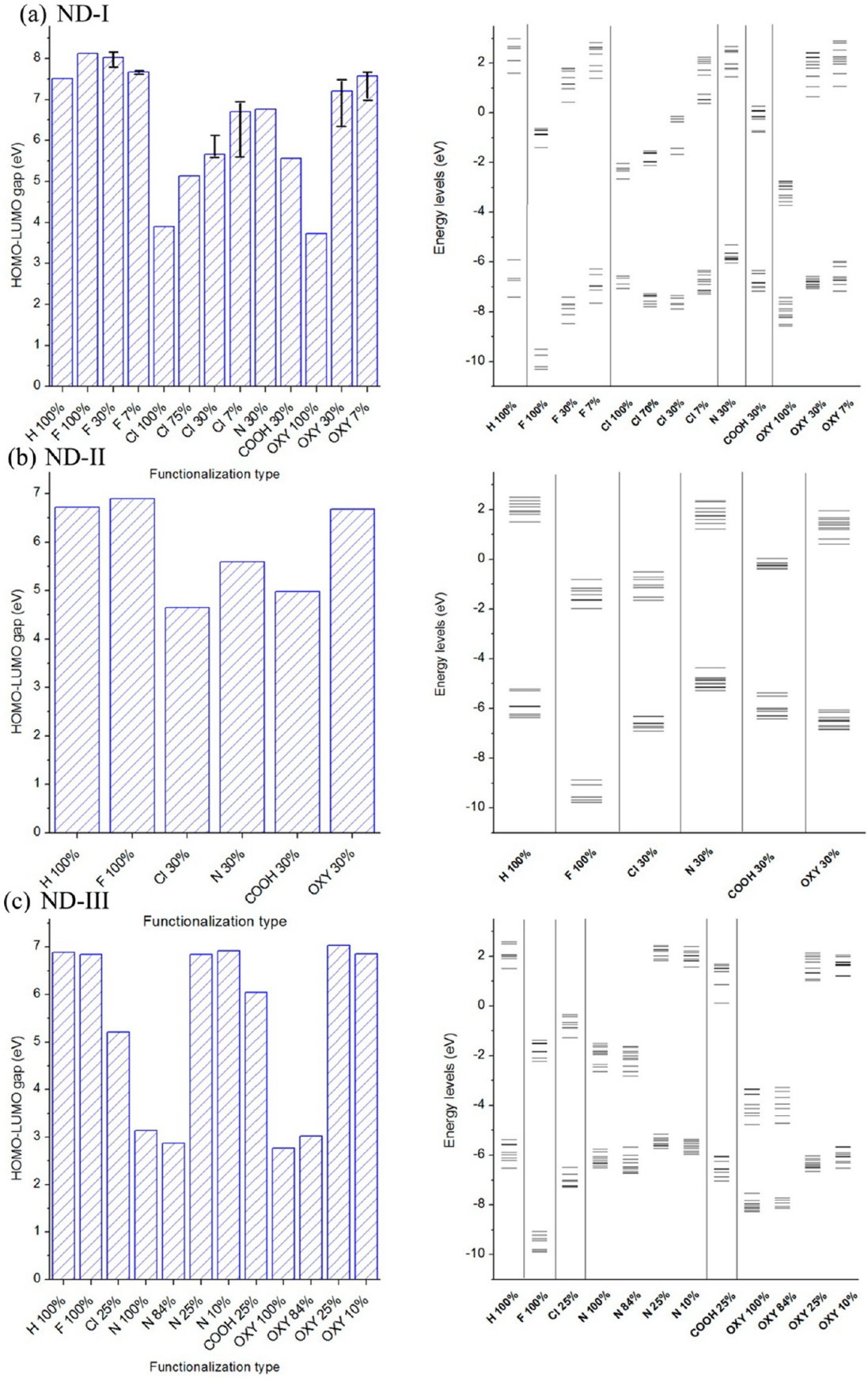

Figure 3. continued

dx.doi.org/10.1021/jp409236t | J. Phys. Chem. C 2014, 118, 5530−5537

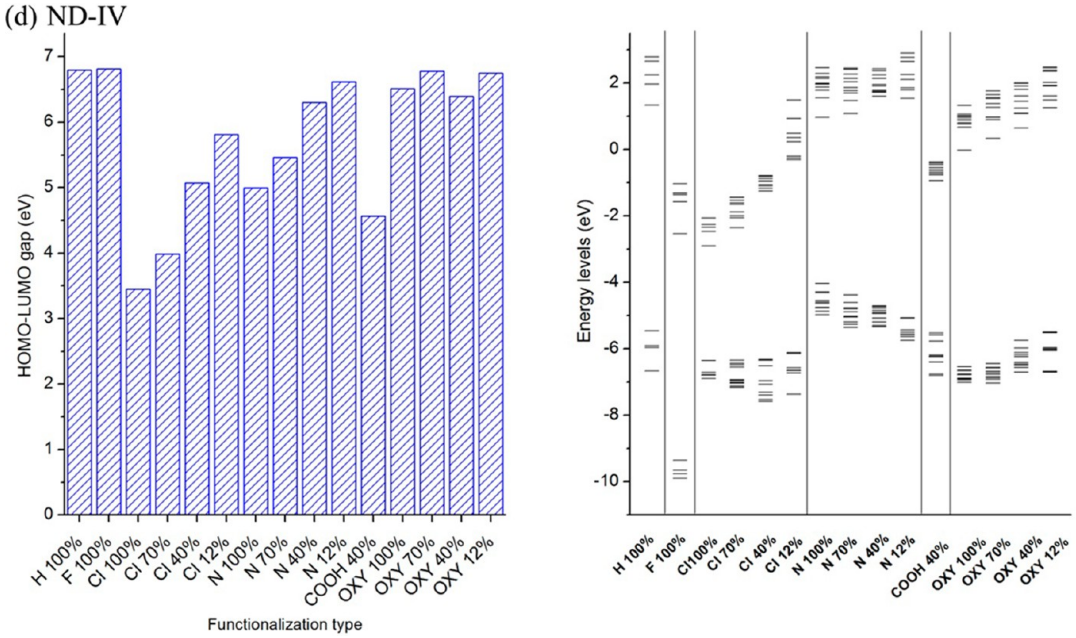

Figure 3. HOMO−LUMO gap (left panels) and graphical representation of the Kohn−Sham eigenvalues spectra (right panels) vs functionalization scheme for (a) ND-I, (b) ND-II, (c) ND-III, and (d) ND-IV as calculated at the HSE/6-31G** level of theory.

7% coverage) with respect to the fully hydrogenated system. Again, this is attributed to the high electronegativity of oxygen. Similar trends are obtained for ND-II, ND-III, and ND-IV (Figure 2b,c,d), apart from the case of high nitrogen coverages (100% and 84%) of ND-III, where steric effects, again, become important. As mentioned above, some high coverage schemes of chlorine, nitrogen, carboxylic acid, and oxygen on ND-II and ND-III could not be obtained due to steric hindrance effects.

Importantly, most of the functionalization schemes studied present negative δG values indicating their relative energetic stability. Results obtained using the LDA and PBE functional approximations show similar trends (see Supporting Information). We therefore deduce that under appropriate synthesis conditions, diverse functionalization designs are expected to occur, which may lead to the formation of new structures presenting varied physical and chemical characteristics.

Electronic Properties. After studying the structural stability of the various nanodiamonds considered, we now turn to evaluate the influence of different functionalization schemes on their electronic properties. Figure 3 presents the dependence of the HOMO−LUMO gap on the type of surface functionalization for the nanodiamond models studied. Concentrating on the HSE results (LDA and PBE results can be found in the Supporting Information), all four fully hydrogenated systems possess a high HOMO−LUMO gap of 6.6−7.5 eV. Despite the strong effect of fluorination on the structural stability of the three nanodiamonds, its influence on the electronic structure is relatively minor showing a maximal 8.2% (0.61 eV) gap increase for ND-I, a smaller gap increase of 2.5% (0.17 eV) for ND-II, and a very small decrease of 0.71% (0.05 eV) and increase of 0.3% (0.02 eV) for the ND-III and ND-IV systems, respectively.

Chlorination, however, results in a strong reduction of the gap in all four systems. Upon gradual decrease of the chlorine density on the ND-I surface the gap is found to increase. Notably, even at the lowest density considered (7%) the HOMO−LUMO gap can be smaller by 25% (1.9 eV) than the fully hydrogenated nanodiamond. The effect of partial (25−40%) carboxylation on the ND-I, ND-II, and ND-IV HOMO−LUMO gaps is similar to that of partial (30−40%) chlorination, whereas for the ND-III system a somewhat smaller gap reduction of 12.2% (0.84 eV) is obtained.

For the nitrogenation functionalization schemes considered we find, again, a relatively small gap decrease of 9.9% (0.74 eV), 16.8% (1.13 eV), 0.64% (0.04 eV), and 7.2% (0.49 eV) for low nitrogen coverages (25−40%) of the ND-I, ND-II, ND-III, and ND-IV systems, respectively. For the fully nitrogenated ND-III system a considerable HOMO−LUMO gap decrease of up to 54.4% (3.75 eV) is obtained, resulting in a 3.14 eV gap semiconducting nanodiamond. Interestingly, an even smaller gap is found for the corresponding 84% nitrogenation scheme. However, for high nitrogen coverages of 70% and 100% of the ND-IV system, lower gap decreases of 19.6% (1.33 eV) and 26.5% (1.80 eV) are seen, respectively.

A very similar trend is found for the oxidation schemes considered, where at high coverage (84−100%) HOMO−LUMO gaps as small as 3.72 and 2.76 eV are obtained for the ND-I and ND-III systems, respectively. At lower oxidation coverages (7−40%) the gap of all four nanodiamonds considered only slightly reduces from that obtained for the fully hydrogenated system. Notably, for the octahedral ND-IV structure, even at high oxygen coverage (70−100%), only small gap variations are obtained.

To better understand this behavior, we plot, on the right panels of Figure 3, the energy levels diagrams of the various systems. Concentrating on ND-I it can be seen that fluorination results in strong downshift of the whole energy spectrum of the system. Nevertheless, since the HOMO and LUMO Kohn−Sham orbital energies are shifted by a similar amount, the overall effect on the HOMO−LUMO gap of the nanodiamond is small. For lower fluorine coverages, the whole eigenspectrum is up-shifted toward that of the hydrogenated system with relatively minor variations of the gap. On the contrary, upon full chlorination there is a strong downshift of the unoccupied

dx.doi.org/10.1021/jp409236t | J. Phys. Chem. C 2014, 118, 5530−5537

subspace and a much weaker effect on the occupied orbitals resulting in the considerable reduction of the HOMO−LUMO gap discussed above. When the chlorine surface coverage is reduced, the unoccupied subspace is gradually up-shifted and the HOMO−LUMO gap approaches that of the fully hydrogenated system. A similar trend is obtained for the oxidation scheme, where full surface coverage results in strong downshift of the unoccupied subspace with gradual recovery of the hydrogenated system spectrum as the surface coverage reduces. The same is true for partial carboxylation, where considerable downshift of the unoccupied subspace and a milder down-shift of the occupied orbital energies results in the reduction of the HOMO−LUMO gap with respect to the hydrogenated systems. On the contrary, for the partially nitrogenated system a small upshift of the HOMO orbital energy with almost no change of the LUMO energy leads to the HOMO−LUMO gap reduction. A similar picture arises for the other nanodiamonds considered indicating the general nature of the effect of various decoration schemes on the electronic properties of these systems and supporting our hypothesis that chemical decoration can be used to tune their electronic properties.

Finally, for the mixed decorated structures, we explore the effect of the exact decoration configuration on the relative stability and electronic properties of the system. To this end, we choose three randomly distributed decoration schemes of the 7% and 30% fluorinated, 7% (Figure 4a−c) and 30%

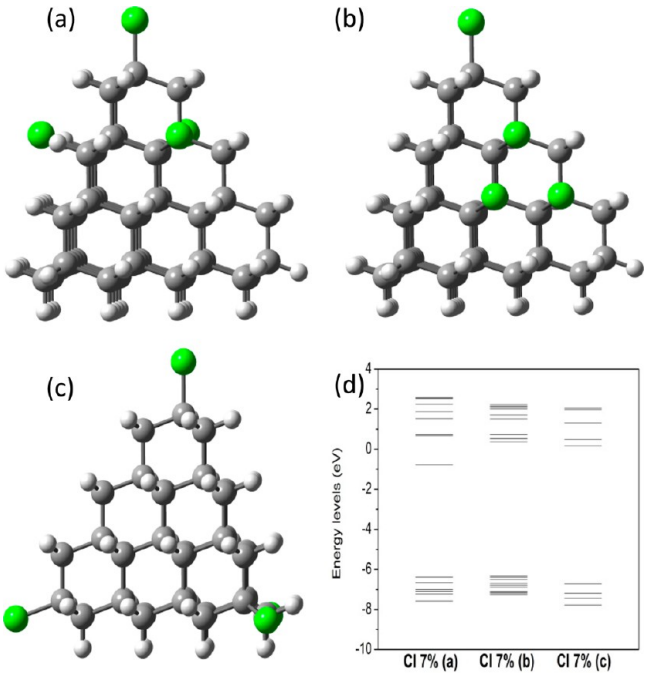

Figure 4. Decoration schemes (a−c) and Kohn−Sham low-energy eigenvalue spectrum (d) for the 7% surface chlorinated ND-I system calculated at the HSE/6-31G** level of theory.

chlorinated, and 7% and 30% (Figure 5a−c) oxidized ND-I structure. Interestingly, we find that, per given atomic surface coverage, the effect of changing the decoration configuration on the relative stability of the system is minor, with changes not exceeding 5%. This may be attributed to the fact that the different decoration configurations, having the same chemical composition, present a very similar chemical bonding scheme.

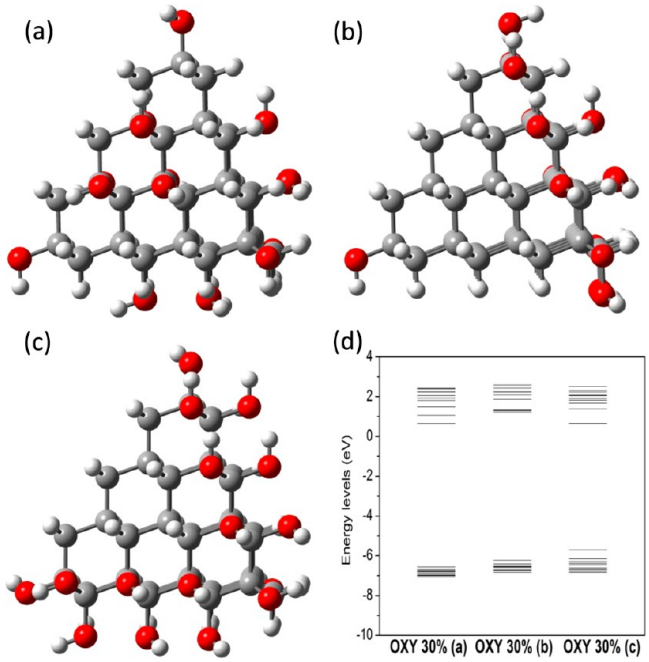

Figure 5. Decoration schemes (a−c) and Kohn−Sham low-energy eigenvalue spectrum (d) for the 30% surface oxidized ND-I system calculated at the HSE/6-31G** level of theory.

A very different picture arises when considering the HOMO−LUMO gap of the various systems. Here, changing the decoration configuration while maintaining a fixed coverage density results in considerable gap variations. As can be seen by the error bars appearing in Figure 3a, for the low-coverage (7%) chlorination scheme the HOMO−LUMO gap can vary by as much as 1.27 eV (which is 19% of the calculated total gap). Similarly, for the 30% coverage oxidation scheme the HOMO−LUMO gap may change by 1.08 eV (15% of the total gap). Somewhat smaller variations were obtained for the 30% chlorination and 7% oxidation schemes. Changing the partial fluorination configuration at a given coverage has an even smaller effect on the gap. To better understand the variations of the HOMO−LUMO gap at a given surface coverage, we plot the energy level diagrams of the ND-I system with the various 7% chlorination (Figure 4d) and 30% oxidation schemes (Figure 5d). As can be seen, the exact decoration scheme has a strong effect both on the density of states in the vicinity of the gap and on the positioning of the HOMO and LUMO energies. This is further reflected by the fact that both HOMO and LUMO orbitals are strongly affected by variations of the decoration scheme as compared to the fully hydrogenated system (Figure 6a−f). Specifically, the LUMO orbitals of the partially decorated systems tend to localize at different apexes, where chemical substitution is introduced.

SUMMARY AND CONCLUSIONS

In this article, we have examined the effect of chemical surface functionalization on the structural and electronic properties of nanodiamonds of different crystal morphologies. Various functionalization schemes have been considered including hydrogenation, fluorination, chlorination, oxidation, nitrogenation, and carboxylation. Most chemical surface decoration schemes considered were found to be energetically stable with respect to their chemical constituents. Specifically, surface fluorination was found to considerably enhance the stability of

dx.doi.org/10.1021/jp409236t | J. Phys. Chem. C 2014, 118, 5530−5537

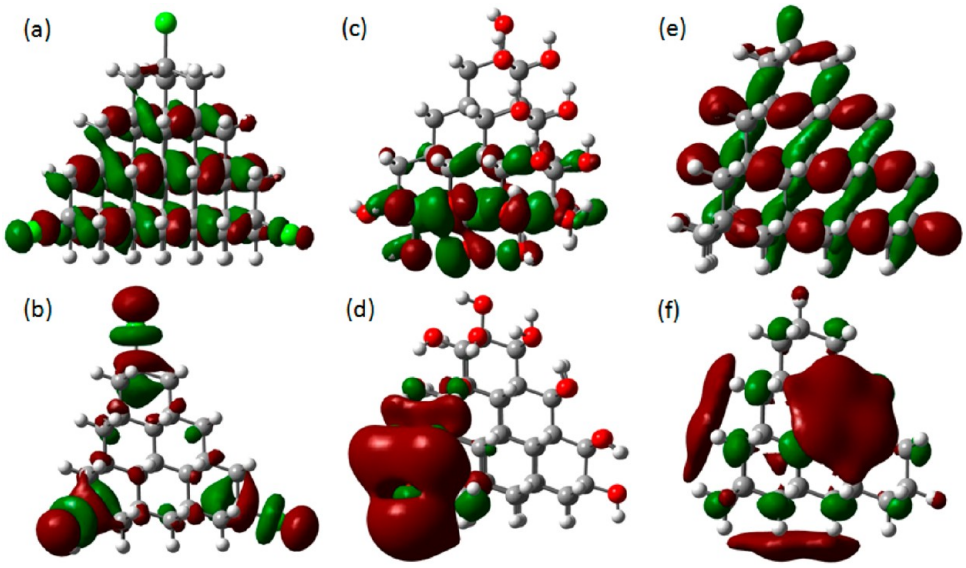

Figure 6. Representative HOMO (upper panels) and LUMO (lower panels) isosurfaces of chosen 7% chlorination (leftmost panels), 30% oxidation (center panels), and full hydrogenation (rightmost panels) schemes of the ND-I system. Similar results are obtained for the other decoration schemes of the various surface coverages. Isosurface value used in these representations is 0.02 electrons/Å^3.

the nanodiamonds resulting in the most favorable structures. Diverse effects of surface chemistry on the electronic structure of the nanodiamonds have been obtained with HOMO−LUMO gaps varying in the range of 2.8−8.1 eV, depending on the morphology of the nanodiamond and its surface functionalization scheme. For the mixed functionalization schemes, it was found that the HOMO−LUMO gap varies gradually with the surface coverage of the decorating groups. Furthermore, at a given surface coverage, the gap was found to be sensitive to the specific decoration scheme. These results suggest that surface chemistry may be used as a viable tool for tailoring the structural stability and electronic properties of carbon-based nanodiamonds.

■ ASSOCIATED CONTENT

Supporting Information

Comparison of the relative stability and electronic structure analyses obtained using the LDA and PBE functional approximations to the HSE results presented in the main text. Relaxed coordinates of the various surface functionalized nanodiamonds considered. This material is available free of charge via the Internet at http://pubs.acs.org.

■ AUTHOR INFORMATION

Corresponding Author

*(O.H.) E-mail: odedhod@tau.ac.il.

Notes

The authors declare no competing financial interest.

■ ACKNOWLEDGMENTS

This work was supported by the Israel Science Foundation under Grant 1313/08, the Center for Nanoscience and Nanotechnology at Tel Aviv University, and the Lise Meitner-Minerva Center for Computational Quantum Chemistry.

■ REFERENCES

(1) Iijima, S. Helical Microtubules of Graphitic Carbon. *Nature* **1991**, *354*, 56−58.
(2) Geim, A. K.; Novoselov, K. S. The Rise of Graphene. *Nat. Mater.* **2007**, *6*, 193−191.
(3) Shemella, P.; Zhang, Y.; Mailman, M.; Ajayan, P. M.; Nayak, S. K. Energy Gaps in Zero-Dimensional Graphene Nanoribbons. *Appl. Phys. Lett.* **2007**, *91*, 042101.
(4) Shenderova, O. A.; Zhirnov, V. V.; Brenner, D. W. Carbon Nanotructures. *Crit. Rev. Solid State Mater. Sci.* **2002**, *27*, 227−356.
(5) Hu, Y.; Shenderova, O. A.; Hu, Z.; Padgett, C. W.; Brenner, D. W. Carbon Nanostructures for Advanced Composites. *Rep. Prog. Phys.* **2006**, *69*, 1847−1895.
(6) Avouris, P.; Chen, Z.; Perebeinos, V. Carbon-Based Electronics. *Nat. Nanotechnol.* **2007**, *2*, 605−615.
(7) Kreupl, F. Electronics: Carbon Nanotubes Finally Deliver. *Nature* **2012**, *484*, 321−322.
(8) Barnard, A. S. Diamond Standard in Diagnostics: Nanodiamond Biolabels Make Their Mark. *Analyst* **2009**, *134*, 1751−1764.
(9) Yu, S.-J.; Kang, M.-W.; Chang, H.-C.; Chen, K.-M.; Yu, Y.-C. Bright Fluorescent Nanodiamonds: No Photobleaching and Low Cytotoxicity. *J. Am. Chem. Soc.* **2005**, *127*, 17604−17605.
(10) Purtov, K. V.; Petunin, A. I.; Burov, A. E.; Puzyr, A. P.; Bondar, V. S. Nanodiamonds as Carriers for Address Delivery of Biologically Active Substances. *Nanoscale Res. Lett.* **2010**, *5*, 631−636.
(11) Bogatyreva, G. P.; Marinich, M. A.; Ishchenko, E. V.; Gvyazdovskaya, V. L.; Bazalii, G. A.; Oleinik, N. A. Application of Modified Nanodiamonds as Catalysts of Heterogeneous and Electrochemical Catalyses. *Phys. Solid State* **2004**, *46*, 738−741.
(12) Mochalin, V. N.; Shenderova, O. A.; Ho, D.; Gogotsi, Y. The Properties and Applications of Nanodiamonds. *Nat. Nanotechnol.* **2012**, *7*, 11−23.
(13) Raty, J.-Y.; Galli, G. Ultradispersity of Diamond at the Nanoscale. *Nat. Mater.* **2003**, *2*, 792−795.
(14) Dolmatov, V. Y. Detonation Synthesis Ultradispersed Diamonds: Properties and Applications. *Russ. Chem. Rev.* **2001**, *70*, 607−626.
(15) Danilenko, V. V. On the History of the Discovery of Nanodiamond Synthesis. *Phys. Solid State* **2004**, *46*, 595−599.
(16) Ugarte, D. Curling and Closure of Graphitic Networks Under Electron-Beam Irradiation. *Nature* **1992**, *359*, 707−709.
(17) Tomita, S.; Sakurai, T.; Ohta, H.; Fujii, M.; Hayashi, S. Structure and Electronic Properties of Carbon Onions. *J. Chem. Phys.* **2001**, *114*, 7477.
(18) Banhart, F. The Transformation of Graphitic Onions to Diamond Under Electron Irradiation. *J. Appl. Phys.* **1997**, *81*, 3440.

(19) Zou, Q.; Li, Y. G.; Lv, B.; Wang, M. Z.; Zou, L. H.; Zhao, Y. C. Transformation of Onion-Like Carbon from Nanodiamond by Annealing. *Inorg. Mater.* **2010**, *46*, 127−131.
(20) Kuznetsov, V. L.; Zilberberg, I. L.; Butenko, Y. V.; Chuvilin, A. L.; Segall, B. Theoretical Study of the Formation of Closed Curved Graphite-Like Structures During Annealing of Diamond Surface. *J. Appl. Phys.* **1999**, *86*, 863.
(21) Barnard, A. S.; Russo, S. P.; Snook, I. K. Structural Relaxation and Relative Stability of Nanodiamond Morphologies. *Diamond Relat. Mater.* **2003**, *12*, 1867−1872.
(22) Barnard, A. S.; Russo, S. P.; Snook, I. K. First Principles Investigations of Diamond Ultrananocrystals. *Int. J. Mod. Phys. B* **2003**, *17*, 3865−3879.
(23) Russo, S. P.; Barnard, A. S.; Snook, I. K. Hydrogenation of Nanodiamond Surfaces: Structure and Effects on Crystalline Stability. *Surf. Rev. Lett.* **2003**, *10*, 233−239.
(24) Wen, B.; Zhao, J.; Li, T. Relative Stability of Hydrogenated Nanodiamond and Nanographite from Density Function Theory. *Chem. Phys. Lett.* **2007**, *441*, 318−321.
(25) Barnard, A. S.; Russo, S. P.; Snook, I. K. Coexistence of Bucky Diamond with Nanodiamond and Fullerene Carbon Phases. *Phys. Rev. B* **2003**, *68*, 073406.
(26) Williams, O. A.; Nesladek, M.; Daenen, M.; Michaelson, S.; Hoffman, A.; Osawa, E.; Haenen, K.; Jackman, R. B. Growth, Electronic Properties and Applications of Nanodiamond. *Diam. Relat. Mater.* **2008**, *17*, 1080−1088.
(27) Barnard, A. S.; Sternberg, M. Can We Predict the Location of Impurities in Diamond Nanoparticles? *Diamond Relat. Mater.* **2007**, *16*, 2078−2082.
(28) Barnard, A. S.; Vlasov, I. I.; Ralchenko, V. G. Predicting the Distribution and Stability of Photoactive Defect Centers in Nanodiamond Biomarkers. *J. Mater. Chem.* **2009**, *19*, 360.
(29) Pichot, V.; Stephan, O.; Comet, M.; Fousson, E.; Mory, J.; March, K.; Spitzer, D. High Nitrogen Doping of Detonation Nanodiamonds. *J. Phys. Chem. C* **2010**, *114*, 10082−10087.
(30) Bradac, C.; Gaebel, T.; Naidoo, N.; Rabeau, J. R.; Barnard, A. S. Prediction and Measurement of the Size-Dependent Stability of Fluorescence in Diamond over the Entire Nanoscale. *Nano Lett.* **2009**, *9*, 3555−3564.
(31) Fokin, A. A.; Tkachenko, B. A.; Gunchenko, P. A.; Gusev, D. V.; Schreiner, P. R. Functionalized Nanodiamonds Part I. An Experimental Assessment of Diamantane and Computational Predictions for Higher Diamondoids. *Chemistry* **2005**, *11*, 7091−7101.
(32) Neugart, F.; Zappe, A.; Jelezko, F.; Tietz, C.; Boudou, J. P.; Krueger, A.; Wrachtrup, J. Dynamics of Diamond Nanoparticles in Solution and Cells. *Nano Lett.* **2007**, *7*, 3588−3591.
(33) Khabashesku, V. N.; Margrave, J. L.; Barrera, E. V. Functionalized Carbon Nanotubes and Nanodiamonds for Engineering and Biomedical Applications. *Diamond Relat. Mater.* **2005**, *14*, 859−866.
(34) Liu, Y.; Gu, Z.; Margrave, J. L.; Khabashesku, V. N. Functionalization of Nanoscale Diamond Powder: Fluoro-, Alkyl-, Amino-, and Amino Acid-Nanodiamond Derivatives. *Chem. Mater.* **2004**, *16*, 3924−3930.
(35) Fokin, A. A.; Schreiner, P. R. Band Gap Tuning in Nanodiamonds: First Principle Computational Studies. *Mol. Phys.* **2009**, *107*, 823−830.
(36) Lai, L.; Barnard, A. S. Stability of Nanodiamond Surfaces Exposed to N, NH, and NH_2. *J. Phys. Chem. C* **2011**, *115*, 6218−6228.
(37) Lai, L.; Barnard, A. S. Modeling the Thermostability of Surface Functionalisation by Oxygen, Hydroxyl, and Water on Nanodiamonds. *Nanoscale* **2011**, *3*, 2566.
(38) Lai, L.; Barnard, A. S. Surface Phase Diagram and Thermodynamic Stability of Functionalisation of Nanodiamonds. *J. Mater. Chem.* **2012**, *22*, 16774−16780.
(39) Hever, A.; Bernstein, J.; Hod, O. Fluorination Effects on the Structural Stability and Electronic Properties of Sp3-Type Silicon Nanotubes. *J. Phys. Chem. C* **2013**, *117*, 14684−146791.
(40) Ushizawa, K.; Sato, Y.; Mitsumori, T. Covalent Immobilization of DNA on Diamond and Its Verification by Diffuse Reflectance Infrared Spectroscopy. *Chem. Phys. Lett.* **2002**, *351*, 105−108.
(41) Fokina, N. A.; Tkachenko, B. A.; Dahl, J. E. P.; Carlson, R. M. K.; Fokin, A. A.; Schreiner, P. R. Synthesis of Diamondoid Carboxylic Acid. *Synthesis* **2012**, *44*, 259−264.
(42) Kohn, W.; Sham, L. J. Self-Consistent Equations Including Exchange and Correlation Effects. *Phys. Rev.* **1965**, *140*, A1133−A1138.
(43) Ceperley, D. M.; Alder, B. J. Ground State of the Electron Gas by a Stochastic Method. *Phys. Rev. Lett.* **1980**, *45*, 566−569.
(44) Perdew, J. P.; Zunger, A. Self-Interaction Correction to Density-Functional Approximations for Many-Electron Systems. *Phys. Rev. B* **1981**, *23*, 5048−5079.
(45) Perdew, J. P.; Burke, K.; Ernzerhof, M. Generalized Gradient Approximation Made Simple. *Phys. Rev. Lett.* **1996**, *77*, 3865−3868.
(46) Perdew, J. P.; Burke, K.; Ernzerhof, M. Generalized Gradient Approximation Made Simple. *Phys. Rev. Lett.* **1997**, *78*, 1396−1396.
(47) Heyd, J.; Scuseria, G. E.; Ernzerhof, M. Hybrid Functionals Based on a Screened Coulomb Potential. *J. Chem. Phys.* **2003**, *118*, 8207−8215.
(48) Heyd, J.; Scuseria, G. E.; Ernzerhof, M. Hybrid Functionals Based on a Screened Coulomb Potential. *J. Chem. Phys.* **2006**, *124*, 219906−219906.
(49) Heyd, J.; Scuseria, G. E. Assessment and Validation of a Screened Coulomb Hybrid Density Functional. *J. Chem. Phys.* **2004**, *120*, 77274−77280.
(50) Heyd, J.; Scuseria, G. E. Efficient Hybrid Density Functional Calculations in Solids: Assessment of the Heyd−Scuseria−Ernzerhof Screened Coulomb Hybrid Functional. *J. Chem. Phys.* **2004**, *121*, 1187−1192.
(51) Hariharan, P. C.; Pople, J. A. The Influence of Polarization Finctions on Molecular Orbital Hydrogenation Energies. *Theor. Chim. Acta* **1973**, *28*, 213.
(52) Francl, M. M.; Petro, W. J.; Hehre, W. J.; Binkley, J. S.; Gordon, M. S.; DeFrees, D. J.; Pople, J. A. Self-Consistent Molecular Orbital Methods. XXIII. A Polarization-Type Basis Set for Second-Row Elements. *J. Chem. Phys.* **1982**, *77*, 3654.
(53) Frisch, M. J.; et al. *Gaussian 09*, revision A.1; Gaussian, Inc.: Wallingford, CT, 2009.
(54) Barone, V.; Hod, O.; Scuseria, G. E. Electronic Structure and Stability of Semiconducting Graphene Nanoribbons. *Nano Lett.* **2006**, *6*, 2748−2754.
(55) Hod, O.; Barone, V.; Peralta, J. E.; Scuseria, G. E. Enhanced Half-Metallicity in Edge-Oxidized Zigzag Graphene Nanoribbons. *Nano Lett.* **2007**, *7*, 2295−2299.
(56) Barone, V.; Hod, O.; Peralta, J. E.; Scuseria, G. E. Accurate Prediction of the Electronic Properties of Low-Dimensional Graphene Derivatives Using a Screened Hybrid Density Functional. *Acc. Chem. Res.* **2011**, *44*, 269−279.
(57) Hod, O.; Peralta, J. E.; Scuseria, G. E. Edge Effects in Finite Elongated Graphene Nanoribbons. *Phys. Rev. B* **2007**, *76*, 233401.
(58) Hod, O.; Barone, V.; Scuseria, G. Half-Metallic Graphene Nanodots: A Comprehensive First-Principles Theoretical Study. *Phys. Rev. B* **2008**, *77*, 035411.
(59) Marom, N.; Bernstein, J.; Garel, J.; Tkatchenko, A.; Joselevich, E.; Kronik, L.; Hod, O. Stacking and Registry Effects in Layered Materials: The Case of Hexagonal Boron Nitride. *Phys. Rev. Lett.* **2010**, *105*, 046801.
(60) Heyd, J.; Peralta, J. E.; Scuseria, G. E.; Martin, R. L. Energy Band Gaps and Lattice Parameters Evaluated with the Heyd-Scuseria-Ernzerhof Screened Hybrid Functional. *J. Chem. Phys.* **2005**, *123*, 174101.
(61) Dumitrică, T.; Hua, M.; Yakobson, B. Endohedral Silicon Nanotubes as Thinnest Silicide Wires. *Phys. Rev. B* **2004**, *70*, 241303.